N94-2414 2

# Toward modeling wingtip vortices

## By O. Zeman

## 1. Motivations and objectives

Wingtip vortices are generated by lifting airfoils; their salient features are compactness and relatively slow rate of decay. The principal motivation for studying the far field evolution of wingtip vortices is the need to understand and predict the extent of the vortex influence during aircraft take-off or landing. On submarines a wingtip vortex ingested into a propeller can be a source of undesirable noise.

The flow field associated with a single vortex freely propagating in the environment is difficult to measure. On an aircraft, the vortices are generated in pairs, and these have a tendency to meander and interact with each other. Environmental conditions such as stratification and ambient turbulence may exert an important influence on the vortex as well. So far, the only quantitative measurements of wingtip vortex (far field) evolution in flight experiments have been reported by Rose & Dee (1963). Wind tunnel experiments of an isolated vortex have been reported by Hoffmann and Joubert (1963), Phillips and Graham (1984), and Bandyopadhyay et al. (1991). In these experiments, a pair of oppositely loaded airfoils have been employed to generate a turbulent vortex with a wake- or jet-like axial flow field. Measurements of trailing vortices behind a lifting hydrofoil (in water) were made by Baker et al. (1974) and Green & Acosta (1991). The near field turbulent structure of a single wingtip vortex has been measured by Zilliac et al. (1993). At present, experimental data of a far-field vortex growth are sparse, and data on turbulence quantities in the vortex are virtually nonexistent. The major difficulty in measuring vortex turbulence is the vortex meander, which results in contamination of turbulence statistics.

The main objectives of this research are i) to establish theoretical understanding of the principal mechanisms that govern the later (diffusive) stages of a turbulent vortex, ii) to develop a turbulence closure model representing the basic physical mechanisms that control the vortex diffusive stage, and further iii) to investigate coupling between the near and far field evolutions; in other words, to study the effect of initial conditions on the vortex lifetime and the ultimate state.

At this stage of the effort, I have concentrated on studying a rectilinear, or line, vortex. Thus, the actual vortex evolution in space downstream from a generating wingtip is replaced by evolution in time. The line vortex is axisymmetric in the mean and treated in cylindrical coordinates, where radial distance and time are the only independent variables. The vortex is assumed to be isolated from external influences and its evolution to be independent of the details of the initial (prescribed) conditions. The influence of different initial conditions will be investigated in future.

When compared with experiments, standard k-$\epsilon$ models are known to overpredict the decay rate of a line vortex. This is due to the absence of the rotation effects

in the turbulence kinetic energy equation. Our past experience with modeling the airflow over hills indicated that a Reynolds stress closure (RSC) model is a must if one is to predict the observed distribution of Reynolds stresses and mean wind on the hilltop. Here, the (convex) streamline curvature can significantly alter the turbulence structure and stress distribution (Zeman and Jensen 1987). We have, therefore, employed a full RSC model where the curvature effects are present intrinsically and appear as explicit terms once the model equations are cast in cylindrical coordinates. As we show later, the RSC model predictions are in broad agreement with the observed line vortex growth, while the $k - \epsilon$ version of the model yields unacceptably high turbulent intensities and vortex growth rates.

The further stages of this research effort are described in the Future Work section of this report.

## 2. Accomplishments

The main accomplishments to date have been the development of a RSC closure model and the theoretical and scaling analysis of the turbulent vortical flow. These accomplishments are described in detail in the forthcoming manuscript (Zeman 1993). The principal result reported here is the model-experiment comparison of the vortex growth rates for different vortex Reynolds numbers. It appears that the mean vortical flow generated by the wingtip very effectively suppresses the Reynolds shear stress which mediates the extraction of energy from the mean flow by turbulence. In consequence, the vortex core growth rate is controlled only by molecular viscosity and the vortex turbulence decays since the turbulence production rate is very nearly zero. This rather unexpected result appears to be supported by experiment as is evident from Figure 1. This section is subdivided in two parts: Model formulation and description and comparison with experiments.

### 2.1 Model formulation and description

The cylindrical coordinates $(r, \theta, z)$ are the natural choice for the Reynolds-averaged description of the turbulent vortex flow. The presence of the pressure-strain and transport terms in the RSC equations requires that the equations be formulated in generalized coordinates $x_i$. Assigning arbitrarily the azimuthal angle $\theta \equiv x_1$, radius $r \equiv x_2$, and axial distance $z \equiv x_3$, we obtain the metric tensors of transformation $g^{ij}, g_{ij}$ whose only nonzero components are $g_{22} = g_{33} = 1$ and $g_{11} = r^2$; the contravariant $g^{\alpha\alpha} = g_{\alpha\alpha}^{-1}$. It is then fairly straightforward but arduous to convert the equations for, say, the contravariant tensor $\overline{u^i u^j}$ to physical, Reynolds stress components in cylindrical coordinates (see e.g. Durbin 1993, also Zeman 1993). Prior to the conversion one must choose an appropriate model for the rapid part $\Pi_{ij}^R$ of the pressure strain term $\Pi_{ij} = \overline{p(u_{i,j} + u_{j,i})}\rho^{-1}$. Here, we employ the general (linear) version of the rapid model proposed by Zeman and Tennekes (1975); written in Cartesian tensor notation the rapid part is

$$\Pi_{ij}^R = 2q^2[\frac{1}{5}S_{ij} + \alpha_1(S_{ik}b_{jk} + S_{jk}b_{ik} - \frac{2}{3}\mathbf{S} \cdot \mathbf{b}\delta_{ij}) + \alpha_2(R_{ik}b_{jk} + R_{jk}b_{ik})]. \quad (1)$$

Here, $b_{ij} = \overline{u_i u_j}/q^2 - \delta_{ij}/3$ is the turbulence anisotropy tensor and $q^2 = \overline{u_j u_j}$ is twice the turbulent kinetic energy (hereon TKE); the mean strain ($\mathbf{S}$) and rotation

(R) tensors are defined as $S_{ij} = \frac{1}{2}(U_{i,j} + U_{j,i})$ and $R_{ij} = \frac{1}{2}(U_{i,j} - U_{j,i})$. The coefficients $\alpha_1$ and $\alpha_2$ can, in principle, be functions of the flow invariants and the turbulence Reynolds number. In practice, $\alpha_1$ and $\alpha_2$ are constant, chosen for the best agreement with experiment. The version of the above model was successfully employed in a boundary layer flow with significant streamline curvature effects (Zeman and Jensen 1987) with $\alpha_1 = 0.375$ and $\alpha_2 = 0.225$.

Labeling the azimuthal, radial, and axial fluctuating velocity components as $u$, $v$, and $w$, respectively, and $U(r,t)$ as the mean azimuthal (vortical) velocity, we can write the set of turbulence model equations as follows:

$$\frac{\partial \overline{u^2}}{\partial t} = 4(1 - \alpha_2)\overline{uv}\frac{U}{r} + 2(1 - \frac{\alpha_1}{3} - \alpha_2)P_s - \Pi_{uu}^s - \frac{1}{r}\frac{\partial}{\partial r}(rT_{uuv}) - \frac{2}{r}T_{uuv} - \frac{2}{3}\epsilon, \quad (2)$$

$$\frac{\partial \overline{v^2}}{\partial t} = -4(1 - \alpha_2)\overline{uv}\frac{U}{r} + 2(\alpha_2 - \frac{\alpha_1}{3})P_s - \Pi_{vv}^s - \frac{1}{r}\frac{\partial}{\partial r}(rT_{vvv}) + \frac{2}{r}T_{uuv} - \frac{2}{3}\epsilon, \quad (3)$$

$$\frac{\partial \overline{w^2}}{\partial t} = \frac{4}{3}\alpha_1 P_s - \Pi_{ww}^s - \frac{1}{r}\frac{\partial}{\partial r}(rT_{wwv}) - \frac{2}{3}\epsilon, \quad (4)$$

$$\frac{\partial \overline{uv}}{\partial t} = 2(1 - \alpha_2)(\overline{u^2} - \overline{v^2})\frac{U}{r} - \{0.4\overline{v^2} + (\alpha_1 - \alpha_2)\overline{u^2} - \frac{2}{3}(\alpha_1 - 0.3)q^2\}r\frac{\partial}{\partial r}(\frac{U}{r})$$

$$-\Pi_{uv}^s - \frac{1}{r^2}\frac{\partial}{\partial r}(r^2 T_{uvv}) + \frac{1}{r}(T_{uuv} - T_{vvv}). \quad (5)$$

In the above equations, $\Pi_{ij}^s = 3.25(\overline{u_i u_j} - \frac{1}{3}q^2\delta_{ij})\epsilon$ stands for the so-called slow return-to-isotropy pressure term, and $T_{ijk} = \overline{u_i u_j u_k}$ are the third moment terms ($u_i$ stands for $u, v, w$). $P_s = -\overline{uv}(\frac{\partial}{\partial r}U - \frac{U}{r})$ is the TKE production rate (by the mean strain $\frac{\partial}{\partial r}U - \frac{U}{r}$). The closure equation for the rate of dissipation used at the present time is in a standard form:

$$\frac{\partial \epsilon}{\partial t} = -3.8(f_1\epsilon - 0.75P_s)\frac{1}{\tau} - \frac{1}{r}\frac{\partial}{\partial r}(rT_{\epsilon v}), \quad (6)$$

with $\tau = q^2/\epsilon$ is the turbulence (equilibrium) time scale and $f_1 = 1 - 0.3\exp(-R_t^2)$ where $R_t = q^4/(9\epsilon\nu)$ is the turbulence Reynolds number.

By summing (2), (3), and (4), the TKE rate equation is obtained

$$\frac{1}{2}\frac{\partial q^2}{\partial t} = P_s - \epsilon - \frac{1}{r}\frac{\partial}{\partial r}(rT_{qqv}). \quad (7)$$

Here $q^2 = \overline{u^2} + \overline{v^2} + \overline{w^2}$ and $T_{qqv} = \frac{1}{2}(T_{uuv} + T_{vvv} + T_{wwv})$ is the (total) flux of $q^2/2$ in the outward radial direction. Note that curvature effects associated with the factor $U/r$ in (2) to (4) are absent in (7).

## 2.1.1. Concerning the transport term model

To first approximation, the third moments $T_{ijk}$ can be considered as radial fluxes of the second-order quantities involved. After some experimentation, we have settled on the following scalar-type, gradient transport model:

$$T_{\phi v} = -(\nu_{tr} + \nu)\frac{\partial}{\partial r}\bar{\phi}, \tag{8}$$

where $\bar{\phi}$ is any second-order quantity in (2)-(7) including $\epsilon$ and the (radial) eddy transport coefficient $\nu_{tr}$ is

$$\nu_{rt} = 0.07\tau\overline{v^2}\frac{1}{1 + d_1\tau^2(K_z^2)'/r^3}. \tag{9}$$

Here, the prime (') stands for radial derivative, and $K_z = Ur = \Gamma/2\pi$ is the angular momentum (in $z$ direction); the adjustable constant $d_1$ is set tentatively at $d_1 = 0.02$. The modification of the eddy coefficient in (9) by the curved flow (stability) parameters is a novel idea, and its rationale is based on the analogous modifications in modeling buoyancy driven flows (Zeman and Lumley 1976). An analogy between streamline curvature and buoyancy has been originally suggested by Bradshaw (1969). Townsend (1976) proposed a curved flow parameter analogous to the gradient Richardson number, i.e.

$$R_{ic} = \frac{(K_z^2)'/r^3}{(U')^2}$$

The modifying factor $(K_z^2)'/r^3$ in (9) is apparently analogous to the Brunt-Vaisaila frequency squared $N^2$ in flows with buoyancy, and the sign of $K_z'$ corresponds to the sign of (potential) temperature in stratified flows. Within the bulk of a turbulent vortex core, $K_z' > 0$, which means turbulence damping.

Donaldson and Sullivan (1971) employed for the modeling of the same (line vortex) flow the invariant transport model

$$\overline{u^i u^j u^k} \propto -\tau(\overline{u^i u^l}(\overline{u^j u^k}),_l + \text{ permutations in } (i,j,k)).$$

The author found this type of model to give unrealistically high levels of the third moments; their effects overwhelmed the solutions. Evidently, the invariant model of Donaldson and Sullivan is incomplete because it does not include curvature (stratification) effects. Ettestad and Lumley (1985) considered the full third-moment equations with the curvature terms included. The resulting transport model was too complex to be applied in actual flow computations, but the modifying factor $\tau^2(K_z^2)'/r^3$ does appear repeatedly in the Ettestad and Lumley expressions for eddy coefficients. Finally, it is interesting that an eddy transport coefficient similar to (9) can also be inferred from a Lagrangian analysis (see Zeman 1993; Ettestad and Lumley 1985). The invariant form of the transport model (8) and (9) for general (non-axisymmetric) flows will be considered in future work (Zeman 1993).

### 2.1.2. Concerning boundary and initial conditions

The boundary conditions at the centerline $r = 0$ are not readily obvious but can be inferred from the following reasoning. If the turbulence undergoes a solid body rotation, the solutions to the equations (2)-(7) must admit a homogeneous solutions independent of $r$. It follows that at $r = 0$,

$$\frac{\partial}{\partial r}\overline{u^2} = \frac{\partial}{\partial r}\overline{v^2} = \frac{\partial}{\partial r}\overline{w^2} = 0 \text{ and } \overline{uv} = 0.$$

The last condition stems from the symmetry requirement. Symmetry also requires that near $r = 0$ the mean flow is solid body rotation and thus $(U/r)' = 0$; this, according to (5), is consistent with $\overline{uv}(r = 0) = 0$ only if $\overline{u^2} = \overline{v^2}$. This centerline turbulence axisymmetry is not directly imposed on the flow, but it is satisfied in actual computations. Similar observations have been reported by Donaldson and Sullivan (1971), who used the same boundary conditions. It is noted that the above boundary conditions are consistent with a theoretical analysis of Shariff (1993) (brought to my attention by Dr. Moser of NASA Ames). Sharif's analysis is based on the requirement that the velocity components $(u, v, w)$ be analytical near $r = 0$. It then follows that near $r = 0$ the components behave as

$$\overline{u^2} = a^2 + b_u r^2 \quad \overline{v^2} = a^2 + b_v r^2, \quad \text{and } \overline{w^2} = c^2 + b_w r^2.$$

Evidently, the turbulence axisymmetry is a requirement of analyticity of the fluctuating flow field at $r = 0$.

The centerline dissipation $\epsilon_c$ is obtained from the integral balance of the TKE equation (7), i. e., $\epsilon_c$ must satisfy the integral

$$\int_0^\infty \{-\frac{1}{2}\frac{\partial \overline{q^2}}{\partial t} + P_s - \epsilon\} r dr = 0. \tag{10}$$

Durbin (1991) showed the integral constraint to give the proper value of $\epsilon$ at the wall in a (steady) channel flow. Here, the situation is somewhat different; the flow is unsteady and near $r = 0$, $q_{,t}^2 = (\nu_{tr} + \nu)q_{,rr}^2 - 2\epsilon_c$.

The conditions at $r \to \infty$ are $\Gamma = \Gamma_o$, (or $U = \Gamma_o/(2\pi r)$), and all second-order turbulence quantities tend to zero. The turbulence time scale $\tau = q^2/\epsilon$ is prescribed to be large (with respect to vortex core time scale) but finite as $r \to \infty$

The initial profile for the azimuthal velocity conditions $U(r, t = 0)$ is given by the prescribed circulation distribution

$$\frac{\Gamma}{\Gamma_o} = 1 - \exp -1.26(r/R_1)^2, \tag{11}$$

where $r = R_1$ is the radius of $max\{U\} = U_1$, and it delimits the size of the vortex core; for the distribution (11) the maximum velocity $U_1$ occurs where $\Gamma = 2\pi U_1 R_1 = 0.716\Gamma_o$. Since the vortex evolution approximately obeys the scaling laws $U_1 \propto (\Gamma_o/t)^{1/2}$ and $R_1 \propto (\Gamma_o t)^{1/2}$, the initially prescribed Reynolds number $\Gamma_o/\nu$

remains constant in time. The Gaussian profile of $\Gamma$ is a laminar vortex solution, or if one assumes the eddy viscosity to be constant, it is a turbulent vortex solution as well (see e.g. Govindaraju & Saffman 1971).

Initial profiles of the turbulence moments were specified as

$$\overline{u^2} = \overline{v^2} = \overline{w^2} = u_o^2 h(r/R_1), \quad \epsilon = u_o^3 r^{-1} h(r/R_1) \text{ and } \overline{uv} = 0,$$

with $h(\eta) = \eta^2 \exp\{1 - \eta^2\}$. The above profiles were fairly consistent with the equation solutions but introduced transient oscillations in the $\overline{uv}$ profiles. The initial turbulence intensity $u_o/U_1$ is a parameter of the flow problem which also specifies the initial turbulence Reynolds number $R_t$. It has been found, so far, that the long-time evolution of the vortex is not very sensitive to the value of $u_o/U_1$ or to the initial spatial distribution of turbulence. However, this aspect will be explored in more detail in future work.

### 2.1.3. Interpretation of the model equations

The equations (2) through (7) have been arranged to highlight the different effects of the mean strain $S = \frac{1}{2}(U' - U/r)$ and rotation $U/r$ on turbulence. According to (7), the turbulence is produced only if the mean strain $S$ is nonzero. The circulation distribution $\Gamma(r)$ in the bulk of a turbulent line vortex remains approximately Gaussian as described by (11), thus $S < 0$ and the shear stress $\overline{uv}$ is positive. Inspection of the equations reveals that for the gradient $K_z' \propto \Gamma' > 0$, the generation of the stress $\overline{uv}$ is severely inhibited and so is the TKE production $P_s = -\overline{uv}S$. In the limit of rapid solid body rotation $U/r = \Omega >> 1/\tau$, equations (2), (3) and (5) yield an oscillatory solution with (inertial wave) frequency $4(1 - \alpha_2)^{1/2}\Omega$. The rapid rotation theories give the frequency of oscillations to be exactly $4\Omega$ (Mansour *et al.* 1991), suggesting that the rapid-pressure model constant $\alpha_2$ should approach zero in the rapid limit $\Omega\tau >> 1$. We found this, however, to be of little consequence for the model results and retained, for the present, the value $\alpha_2 = \alpha_1 = 0.3$ inferred from realizability considerations (Zeman 1981). By comparing the TKE equation (7) with the RSC equations (2)-(5), one can easily see that the rotational terms (associated with $U/r$) are absent in the TKE equation showing that, as alluded to earlier, standard $k - \epsilon$ models cannot represent the stabilizing effect of the concentrated vortex flow. Results supporting this conjecture are presented in the following section.

### 2.3. Computations, comparison with experiments

The most important result of the present work is contained in Figure 1. Here, the vortex core growth parameter

$$b_1 = \frac{\Delta(R_1)}{\Delta(\Gamma_o t)^{1/2}} \tag{12}$$

is plotted against the flow Reynolds number $\Gamma_o/\nu$. The observation data points plotted are a mixture of flight and laboratory experiments as indicated in the figure legend. There are two set of model results; one computed with the present RSC
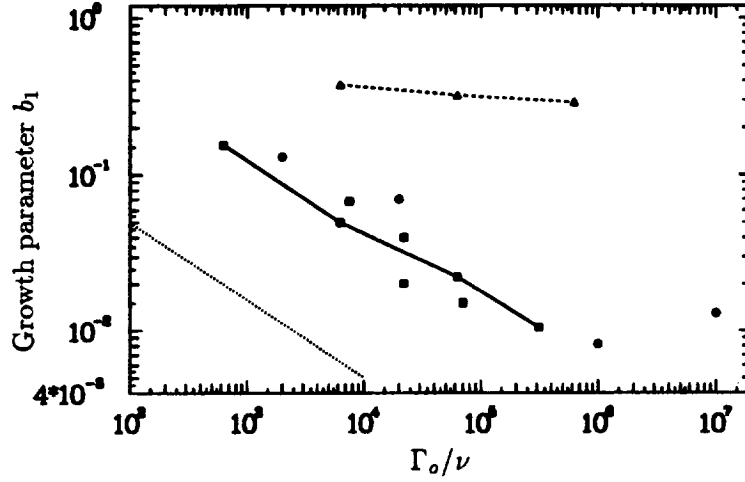
FIGURE 1.   Vortex core growth rate $b_1$ (defined in (12)) vs $\Gamma_o/\nu$. Data compiled in Govindraju and Saffman (1971): ● ; Baker *et al.* (1974): ■ ; RSC model results: □ —— □ ; $k - \epsilon$ model: △ ---- △ ; $-1/2$ slope: ········ .

model, and the second with a $k - \epsilon$ model. The $k - \epsilon$ model consists of equations (6), (7), and the constitutive relation for the stress $\overline{uv}$

$$\overline{uv} = -\frac{\nu_{T_o}}{1 + c_1 r^2 (K_z')^2 / r^3} \left( \frac{\partial}{\partial r} U - \frac{U}{r} \right).$$
(13)

In (13) $\nu_{T_o}$ is the standard eddy viscosity for curvature-free flows. The curvature effect on the eddy viscosity is included through a modification similar to (9). Without this modification, the computed turbulence levels and vortex core growth rates were hopelessly unrealistic. Even so, as shown in Figure 1, the growth rate parameter $b_1$ computed with the modified $k - \epsilon$ model is still an order of magnitude higher then indicated by experiments or the RSC model. This trend could not be significantly altered by increased damping through the constant $c_1$.

The present results, although still tentative, have some surprising implications. First, as seen in Figure 1, the experimental growth parameter $b_1$ appears to follow a trend $b_1 \propto (\Gamma_o/\nu)^{-1/2}$ which suggests viscous rather than turbulent diffusion of the vortices. In other words, it suggests a dependence

$$R_1 \propto (\nu t)^{1/2} \propto (\Gamma_o/\nu)^{-1/2} (\Gamma_o t)^{1/2}.$$

This trend is evidently reproduced by the RSC model results. Indeed, the inspection of computed stress profiles show that the turbulent shear stress $\overline{uv}$ is so effectively damped by the swirl that within the vortex core the angular momentum transfer is dominated by the viscous stress. Whatever turbulence is present throughout the vortex, it is passive and does not contribute to the momentum transfer, except in the outer part of the vortex $2R_1 < r < 3R_1$. Hence, the RSC-computed vortex appears to be quasi-laminar. On the other hand, the same vortex predicted by the
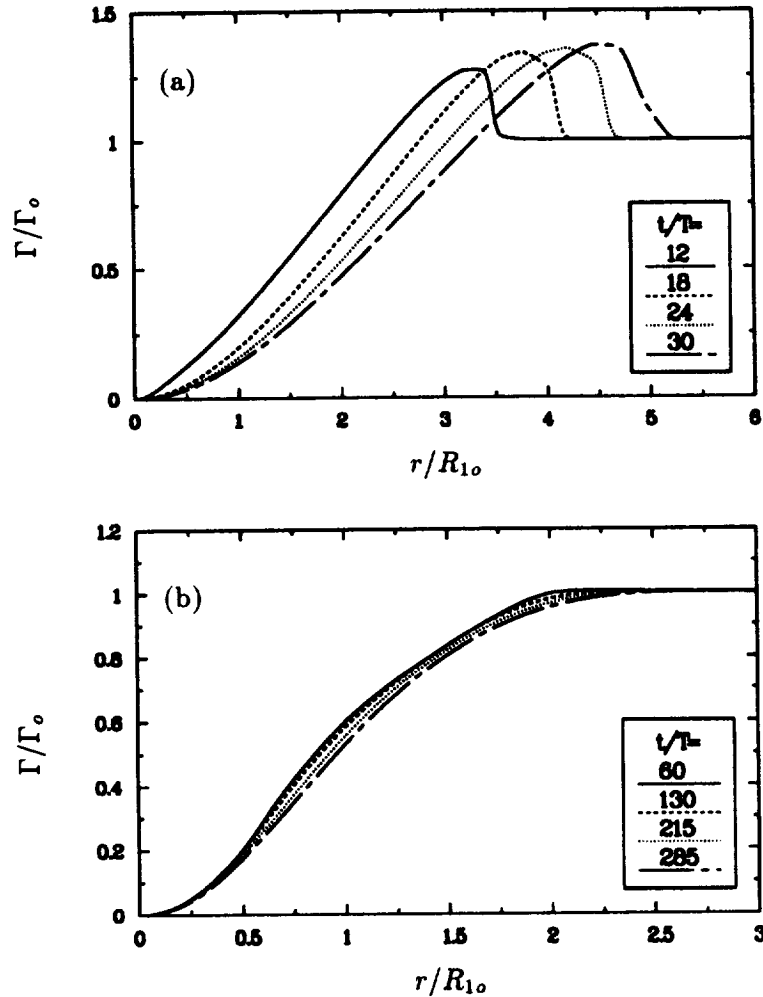
FIGURE 2.   Circulation profile evolution computed by: (a) $k - \epsilon$ model, (b) RSC model; the indicated time of evolution $t$ is in units of $T = (R_1/U_1)_o$.

$k - \epsilon$ model is fully turbulent within the core and the angular momentum transfer is dominated by turbulence. Thus as indicated in Figure 1, the growth parameter $b_1$ inferred from the $k - \epsilon$ model results is independent of $\Gamma_o/\nu$.

The second result of interest is the circulation profile evolution. As seen in Figure 2, there is a striking difference between the $\Gamma$ profile evolutions computed by the RSC and $k - \epsilon$ models. The fully turbulent vortex computed by the $k - \epsilon$ model develops an overshoot in circulation, while the quasi-laminar vortex computed by the RSC model evolves on the viscous time scale and changes very little within the time period shown. Both of these results are consistent with the analysis of Govindraju and Saffman (1971). They inferred from the equations of motion that

for a turbulent vortex, the nondimensional quantity

$$I_\gamma = \frac{1}{R_1^2} \int_0^\infty \frac{\Gamma_o - \Gamma}{\Gamma_o} r\,dr$$

should approach zero for sufficiently large times $t >> R_1^2/\Gamma_o$, and thus the $\Gamma$ distribution should develop an overshoot. Evidently this is true for the $k - \epsilon$ model as shown in Figure 2a. On the other hand, a lack of a visible overshoot (about 1% of $\Gamma_o$) in Figure 2b, indicates that $I_\gamma$ remains approximately constant and this result is again consistent with the quasi-laminar vortex computed by the RSC model.

In conclusion, on the basis of experimental evidence presented in Figure 1, we have inferred that the vortex growth is dominated by viscous effects and not by turbulence. This view is consistent with the RSC model results, which suggest that the turbulent momentum transfer is suppressed by the stabilizing effect of the swirl and that the vortex turbulence plays only a passive role in the vortex dynamics.

## 3. Future work

The modeling results are sufficiently interesting to continue exploring the wingtip vortex modeling in the present geometry. There are many questions to be answered before proceeding to a more complex flow configuration which allows for an axial shear and pressure gradient. It has to be established whether the computed quasi-laminar vortex is a representation of physics, or whether it is an artifact of the RSC model. To this end, we shall test different model versions, investigate the effect of initial conditions, and make more detailed model-experiment comparisons.

## Acknowledgements

## REFERENCES

BAKER, G. R., BARKER, S. J., BOFAH, K. K., & SAFFMAN, P.G. 1974 Laser anemometer measurements of trailing vortices in water. *J. Fluid Mech.* **65**, 325-336.

BANDYOPADHYAYA, P. R., STEAD, D. J.& ASH, R. L. 1991 Organized nature of a turbulent trailing vortex. *AIAA J.* **29**, 1627-1633.

BRADSHAW, P. 1969 The analogy between streamline curvature and buoyancy in turbulent shear flows. *J. Fluid Mech.* **36**, 177-192.

DONALDSON, C. DUP. & SULLIVAN, D. 1971 Decay of an isolated vortex. *Aircraft Wake Turbulence and its Detection.* Ed. J. H. Olsen and A. Goldberg, Plenum Press 1971.

DURBIN, P. 1993 A Reynolds stress model for near-wall turbulence. *J. Fluid Mech.* **249**, 465-498.

DURBIN, P. 1991 Near-wall turbulence closure modeling without "damping functions". *Theoret. Comput. Fluid Dyn.* **3**, 1-13.

ETTESTAD, D. & LUMLEY, J. L. 1985 Parameterization of turbulent Transport in swirling flows. *Turbulent Shear Flows 4*. Eds: Bradbury *et al.*, Springer-Verlag.

GOVINDARAJU & SAFFMAN, P.G. 1971 Flow in a turbulent trailing vortex. *Phys. Fluids.* **14**, 2074-80.

GREEN, S. A.,& ACOSTA, A. J. 1991 Unsteady flow in trailing vortices. *J. Fluid Mech.* **227**, 107-134.

HOFFMANN, E. R. & JOUBERT, P. N. 1963 Turbulent line vortices. *J. Fluid Mech.* **16**, 395-411.

PHILLIPS, W. R. C. & GRAHAM, J. A. H. 1984 Reynolds stress measurements in a turbulent trailing vortex. *J. Fluid Mech.* **147**, 353-71.

ROSE, R. & DEE, W. F. 1965 Aircraft vortex wake and their effects on aircraft. *Aeron. Res. Council.* CP 795.

SHARIFF, K. 1993 Comments on "Coordinate singularities" by P. R. Spalart, Unpublished note.

TOWNSEND, A. A. 1976 *The structure of turbulent shear flows.* Cambridge University Press, pp 429.

ZILLIAC, G. G., CHOW, J.S., DACLES-MARIANI, J., & BRADSHAW, P. 1993 Turbulent structure of a wingtip in the near field. *AIAA Paper 93-3011.* 24nd Fluid Dynamics Conference, Orlando, Florida.

ZEMAN, O. 1981 Progress in the modeling of planetary boundary layers. *Ann. Rev. Fluid Mech.* **13**, 253-72.

ZEMAN, O. 1993 Toward modeling wingtip vortices. In preparation.

ZEMAN, O., & TENNEKES, H. 1975 A self-contained model for pressure terms in the turbulent stress equation. *J. Atmos. Sci.* **32**, 1808-13.

ZEMAN, O., & LUMLEY, J. L. 1976 Modeling buoyancy driven mixed layers. *J. Atmos. Sci.* **33**, 1974-88.

ZEMAN, O., & JENSEN, N. O. 1987 Modification of turbulence characteristics in flows over hills. *Q. J. Roy. Meteorol. Soc.* **113**, 55-80.